Taylor & Francis
Taylor & Francis Group

International Geology Review

ISSN: 0020-6814 (Print) 1938-2839 (Online) Journal homepage: http://www.tandfonline.com/loi/tigr20

Contact Metamorphism of the Daulet Suite by Solid-State Emplacement of the Kokchetav UHP-HP Metamorphic Slab

Masaru Terabayashi , Tsutomu Ota , Hiroshi Yamamoto & Yoshiyuki Kaneko

To cite this article: Masaru Terabayashi , Tsutomu Ota , Hiroshi Yamamoto & Yoshiyuki Kaneko (2002) Contact Metamorphism of the Daulet Suite by Solid-State Emplacement of the Kokchetav UHP-HP Metamorphic Slab, International Geology Review, 44:9, 819-830, DOI: 10.2747/0020-6814.44.9.819

To link to this article: http://dx.doi.org/10.2747/0020-6814.44.9.819

Published online: 14 Jul 2010.

International Geology Review, Vol. 44, 2002, p. 819–830.

Contact Metamorphism of the Daulet Suite by Solid-State Emplacement of the Kokchetav UHP-HP Metamorphic Slab

MASARU TERABAYASHI,[1]

Department of Safety Systems Construction Engineering, Kagawa University, Kagawa 761-0396, Japan

TSUTOMU OTA,

Department of Earth and Planetary Sciences, Tokyo Institute of Technology, Tokyo 152-8551, Japan

HIROSHI YAMAMOTO,

Department of Earth and Environmental Sciences, Kagoshima University, Kagoshima 890-0065, Japan

AND YOSHIYUKI KANEKO

AIST Research Fellow, Geoscience and Technology, Geological Survey of Japan,
National Institute of Advanced Industrial Science and Technology, Tsukuba 305-8567, Japan

Abstract

The andalusite-sillimanite–type low-pressure Daulet Suite underlies the Kokchetav ultrahigh-pressure–high-pressure (UHP-HP) massif of northern Kazakhstan. The Daulet Suite is composed of pelitic-psammitic gneisses or schists and quartz schist with minor amounts of metacarbonate and metabasite. About 300 thin sections were examined from the Daulet metapelites; rocks were divided into two mineral zones. Zone A is characterized by andalusite + cordierite + biotite, and zone B by sillimanite + cordierite + biotite with excess K-feldspar, quartz, and plagioclase in both zones. K-feldspar appears with andalusite at lower temperatures than the first formation of sillimanite. Pressure-temperature conditions of the Daulet metamorphism range from 580 to 680°C at a nearly constant pressure of ~2 kbar. Comparison of compositions of solid-solution minerals with a buffered assemblage indicates that the metamorphic grade increases towards the boundary with the overlying UHP-HP unit. Detailed mapping revealed that the primary structure of both the Kokchetav UHP-HP massif and its surrounding units is subhorizontal; the UHP-HP unit has been thrust over the Daulet Suite with a top-to-the-north movement. The thermal structure of the Daulet Suite is subhorizontal and metamorphic grade increases upwards—i.e., toward the boundary with the UHP-HP unit—whereas the thermobaric maximum of the UHP-HP unit occurs at an intermediate structural level. The upward increase in metamorphic grade within the Daulet Suite implies contact metamorphism by the tectonic juxtaposition of the "hot" Kokchetav UHP-HP unit at shallow crustal levels.

Introduction

CONTACT OR THERMAL metamorphism results from a rise in temperature in surrounding country rocks near igneous intrusions (Yardley, 1989). Fluids circulating around the intrusions also play a significant role in contact metamorphism. An igneous intrusion commonly produces a relatively narrow metamorphic aureole with concentric isotherms around it. On the other hand, it is known that overthrusting of metamorphic units in collisional belts produces an inverted metamorphic gradient in the underlying unit. In the Himalayan orogen, the metamorphic core exists in the structural middle Higher Himalayan Sequence, and so-called "inverted metamorphism" has been observed in the underlying Lesser Himalayan Sequence (Gansser, 1964). Le Fort (1975, 1986) proposed that thrusting of the "hot" Higher Himalayan Sequence over the Lesser Himalayan Sequence and Midland Zone along the Main Central Thrust resulted in downbuckling of the isotherms along the Main Central Thrust. The "hot-iron" model would have been coupled with downward conductive heating of the Lesser Himalayan Sequence, with cooling of the hanging wall in the Higher Himalayan Sequence. Hodges et al. (1996) considered that the Main Central Thrust system is a high-strain zone that is a few kilometers thick.

[1]Corresponding author; email: tera@eng.kagawa-u.ac.jp

Kaneko (1997) reported steep increases in metamorphic temperature in the Lesser Himalayan Sequence just below the Main Central Thrust. To produce the inverted metamorphic gradient, several different ideas have been proposed, such as the effects of radioactivity both within the thrust complex and the underlying unit (Oxburgh and Turcotte, 1974) and shear heating along boundary faults (England and Molnar, 1993).

The Kokchetav massif of northern Kazakhstan consists of UHP and HP units, and its geological and thermobaric structures are subhorizontal (Kaneko et al., 2000; Ota et al., 2000). The Daulet Suite underlies the UHP-HP unit beneath a thrust dipping to the north. It has been considered that the Daulet Suite was metamorphosed by extensive Late Ordovician–Early Silurian granite intrusions (Dobretsov et al., 1995; Shatsky et al., 1995). Mineral parageneses in the Daulet metapelites systematically change toward the boundary between the UHP-HP unit during prograde metamorphism of low-P/T–type andalusite-sillimanite series, suggesting that the underlying Daulet Suite was metamorphosed by solid intrusion of a "hot" UHP-HP metamorphic slab. The weakly metamorphosed underlying unit is rich in hydrous phases, hence large amounts of water-rich fluids were available to modify the UHP-HP mineralogy by hydration reactions, when the UHP-HP unit was thrust over the lower unit. Tectonic juxtaposition of the anhydrous UHP-HP unit upon the hydrous low-grade rocks would allow infiltration of fluid into the UHP-HP unit (Terabayashi et al., 1999). Accordingly, most ultrahigh-pressure minerals are selectively replaced by Barrovian-type mineral assemblages.

In this study, mineral assemblages in metapelites of the Daulet Suite underlying the Kokchetav UHP-HP massif, and compositional changes of solid-solution minerals in buffered assemblages were studied. The P-T conditions of the Daulet metamorphism and the amount of dehydrated fluid from the Daulet Suite were estimated.

Geologic Outline

The Kokchetav UHP-HP massif in the southern Siberian steppes, northern Kazakhstan, occupies an area of approximately 30×150 km^2. The Kokchetav UHP-HP metamorphic rocks are composed of Precambrian rocks overlain by the Cambro-Ordovician volcanic and sedimentary rocks of mainly island-arc series, Devonian volcanic molasse, and Carboniferous and Triassic shallow-marine and lacustrine deposits (Dobretsov et al., 1995). The Kokchetav UHP-HP unit has been divided into four fault-bounded lithological units: I, II, III, and IV from the bottom to the top (Kaneko et al., 2000; Fig. 1). Unit I is composed mainly of alternating siliceous schist and amphibolite. Unit II is composed chiefly of pelitic-psammitic gneiss with locally abundant eclogite boudins (mostly amphibolitized) and whiteschist. Unit III consists of alternating felsic gneiss and amphibolite, locally with large eclogite blocks. Unit IV consists mainly of quartzite and siliceous schist. The primary structure appears to be subhorizontal and the total thickness of the UHP rocks is estimated at around 2 kilometers. The first-order structure is sandwich-like—i.e., the UHP-HP unit is separated from both underlying low-P/T metamorphic rocks of the Daulet Suite and overlying unmetamorphosed to feebly metamorphosed sedimentary strata (unit V) by subhorizontal faults (Kaneko et al., 2000). These two major sharp tectonic boundaries are locally modified by secondary high-angle normal and/or strike-slip faults. The Kokchetav massif and Daulet Suite were intruded by Early Devonian syn-collisional granites and Late Devonian to Carboniferous post-collisional granites (Dobretsov et al., 1995).

The Kokchetav UHP-HP metamorphic rocks are bounded to the south by the Daulet Suite, which consists predominantly of pelitic-psammitic gneiss and schist with cordierite-biotite-andalusite/sillimanite parageneses, and intercalations of quartz schists, marble, and rare basic schists. In the Chaglinka, Sulu-Tjube, and Kulet areas, the Daulet Suite is in thrust contact with the southern margin of the UHP-HP unit (Fig. 2). Ishikawa et al. (2000) investigated the relationship between the UHP-HP unit and the Daulet Suite in the Sulu-Tjube area. The UHP-HP unit overlies the Daulet Suite across a NW-dipping subhorizontal thrust. Kinematic indicators show top-to-the-north sense of shear along the thrust. The boundary thrust is partly cut by N-S–trending high-angle faults, related to the post-collisional granitic intrusions.

Metamorphic Zonation

About 300 thin sections of metapelites were examined to delineate metamorphic isograds in the Daulet Suite in the eclogite-rich Chaglinka, Sulu-Tjube, and Kulet areas (Table 1). As a result, two mineral zones A and B were mapped in the above

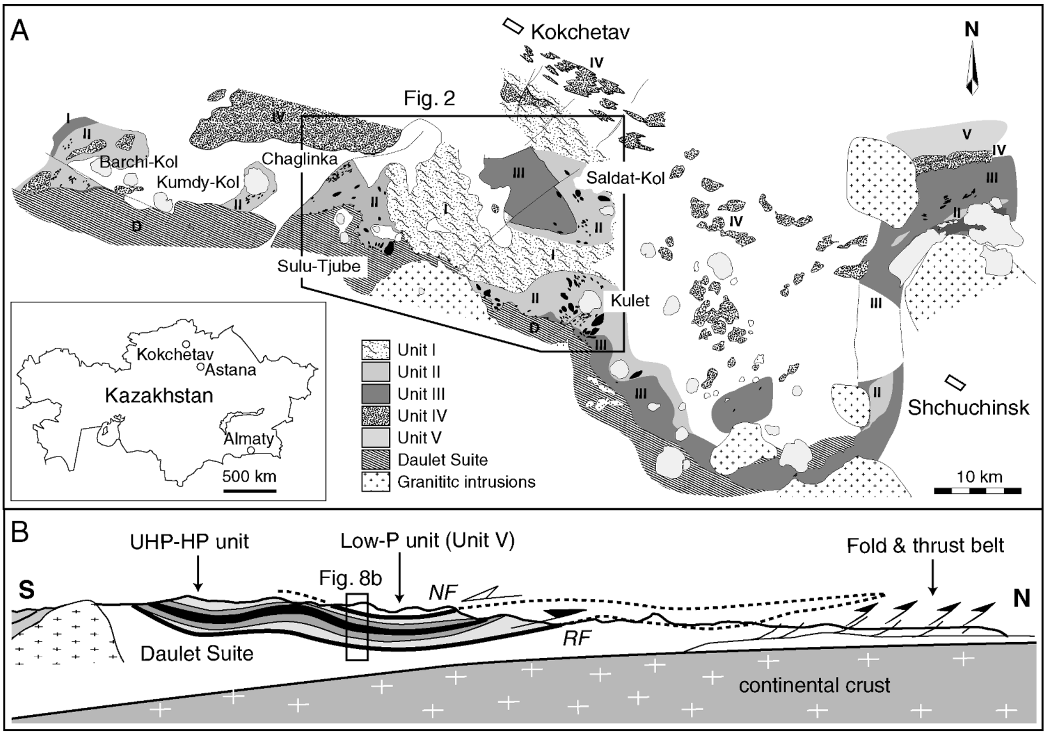

FIG. 1. A. Simplified geologic map of Kokchetav UHP-HP massif showing the major tectonostratigraphic divisions, after Kaneko et al. (2000). The approximate location of the geologic map enlarged in Figure 2 is shown. B. Simplified cross-section of the Kokchetav orogenic belt.

areas (Fig. 3). Sillimanite-bearing metapelite appears near the boundary thrust between the UHP-HP unit. Schematic mineral parageneses for the Daulet metapelites are shown in Figure 4. Heavy lines show major phases and dashed lines show minor and trace phases. Zone A is characterized by the assemblage andalusite + biotite + cordierite + K-feldspar, whereas zone B is defined by the appearance of sillimanite as fibrolite. Andalusite occurs throughout both zones but is missing from some samples. Polycrystalline muscovite forms a corona between andalusite porphyroblast and biotite (Fig. 5A). Andalusite grains are surrounded by a cordierite aggregate, some with the same optical orientation, suggesting they were originally a single grain (Fig. 5B). Sillimanite usually occurs as an aggregate of fibrous crystals surrounded by cordierite (Fig. 5C). Small cordierite neoblasts occur with biotite (Fig. 5D). Biotite, K-feldspar, plagioclase, and quartz are common in both zones. Hercynite occurs in zones A and B as inclusions in cordierite. Most opaques are ilmenite. Titanite rims ilmenite and probably is of retrograde origin in these mineral assemblages. Muscovite is also considered as a secondary phase, judging by its texture. Almost decomposed garnet and stourolite were observed in several specimens, and are regarded as unequilibrated phases.

Boundaries between zones A and B are subparallel to the boundary thrust between the Daulet Suite and the Kokchetav UHP-HP unit; the metamorphic grade in the Daulet metapelites increases towards the boundary. In the Kulet area, the metamorphic zone boundary is not concentric around the Devonian granitoid, and in the farthest part of the Daulet Suite from the boundary thrust, mineral assemblages with aluminum-silicates are less common (Fig. 3C). Distinctive crystallization in the Daulet Suite begins at temperatures where both biotite and cordierite are stable, and metamorphic grade does not increase toward the plutonic intrusion.

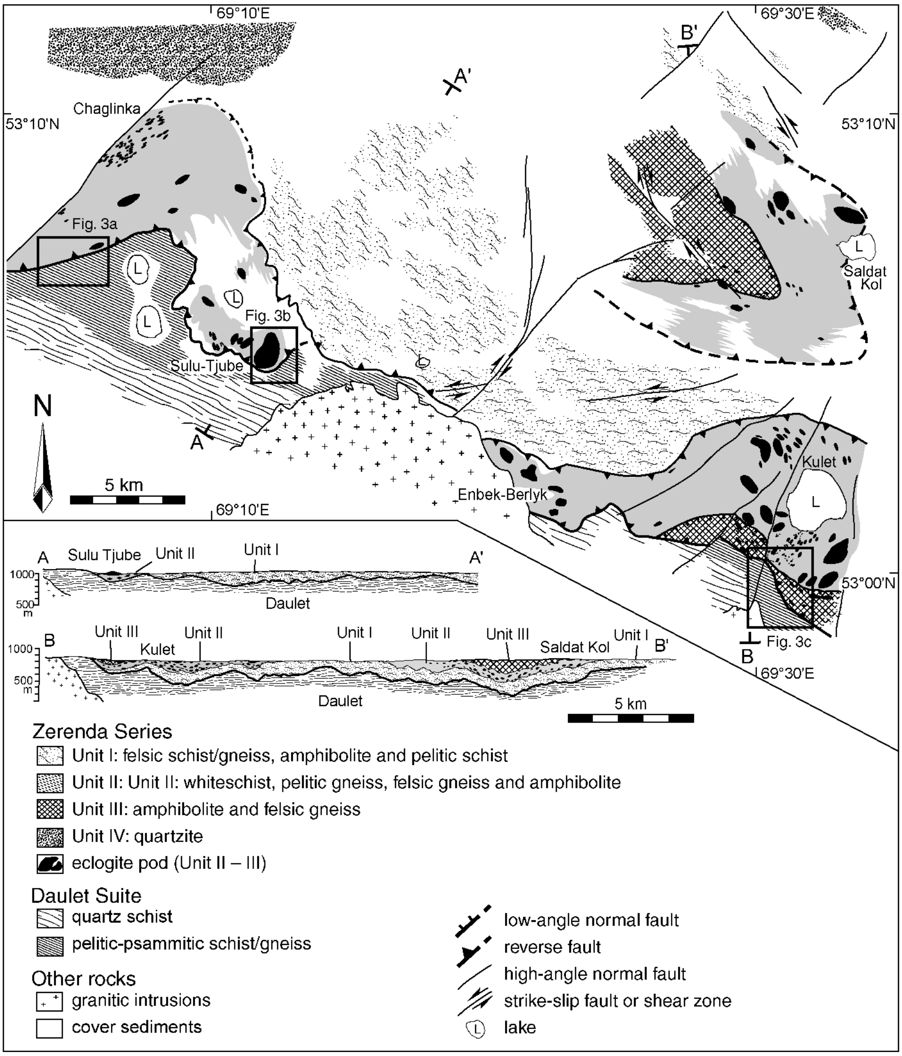

FIG. 2. Geologic map of the Chaglinka-Kulet area after Yamamoto (2000). The Kokchetav UHP-HP metamorphic belt is structurally overlain by a low-grade metamorphic unit on the top, and is underlain by the Daulet Suite of the low-pressure facies series. These two major sharp tectonic boundaries are subhorizontal, and locally modified by secondary high-angle normal faults. Post-orogenic intrusions of Devonian granitoids occupy the southern part of the study area.

Mineral Chemistry and P-T Conditions

Mineral compositions were analyzed using a JEOL electron-probe microanalyzer JXA-8800R with a wavelength-dispersive system at Naruto University of Education. Accelerating voltage, beam current, and beam diameter for quantitative analyses were kept at 15 kV, 15 nA on the Faraday cup, and 3 μm, respectively. X-ray intensities were reduced using a ZAF matrix correction scheme. Representative analyses of biotite, cordierite, and K-feldspar in analyzed samples are shown in Tables 2 and 3. Detailed tabulated mineral compositions are available from the first author. Mineral abbreviations are after Kretz (1983).

Mineral compositions of 13 metapelites from the Kulet area were analyzed by microprobe; locations of analyzed samples are shown in Figure 3C. Biotite

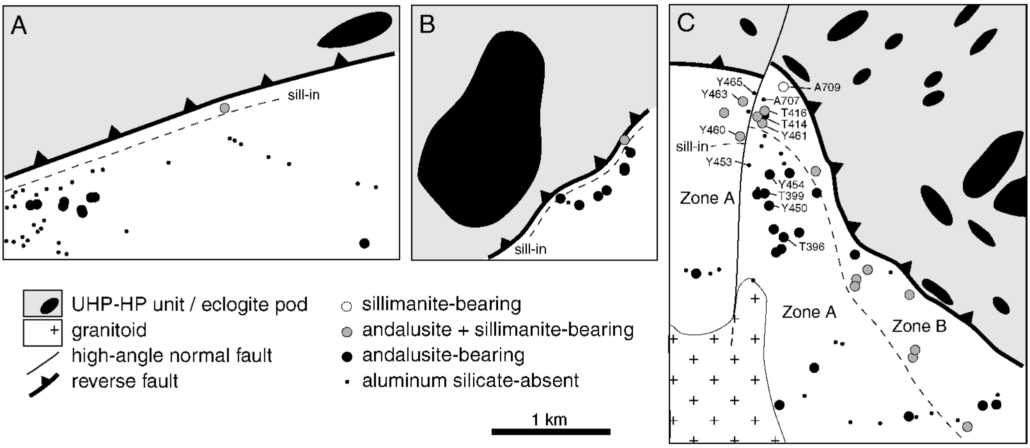

FIG. 3. Metamorphic zonation map of the Daulet metapelites based on mineral assemblages in the (A) Chaglinka, (B) Sulu-Tjube, and (C) Kulet areas. The Daulet Suite is tectonically overlain by the UHP-HP units and intruded by Devonian granitoids. Metamorphic grade increases structurally upward.

TABLE 1. Constituent Minerals in Samples Examined from the Daulet Suite[1]

Zone	Sample no.	Sil	And	Bt	Crd	Kfs	Pl	Qtz	Ilm	Hel
A	T396		+	+	+	+	+	+		+
A	Y450		+	+	+	+	+	+	+	
A	T399		+	+	+	+	+	+	+	+
A	Y454		+	+	+	+	+	+	+	
A	Y453		+	+	+	+	+	+		+
B	Y460	fib	+	+	+	+	+	+	+	+
B	Y461	fib	+	+	+	+	+	+	+	
B	T414		+	+	+	+	+	+	+	
B	T416	fib	+	+	+	+	+	+		
B	A707		+	+	+	+	+	+	+	
B	Y463	fib	+	+	+	+	+	+		
B	Y465			+	+	+	+	+		+
B	A709	+		+		+	+	+		

[1]Locations of the listed samples are shown in Figure 3C.

compositions of the buffered assemblage cordierite + biotite + aluminous silicate from both zones are shown in Figure 6. The tschermak substitution [(Fe,Mg)SiAl$_{-2}$] in biotite does not show consistent variation with metamorphic grade, but a significant increase in XMg from zone A to zone B was observed. Mineral reactions responsible for these changes can be treated in the K_2O–FeO–MgO–Al_2O_3–SiO_2–H_2O (KFMASH) model pelitic system and its subsystems. Changes of XMg with increasing metamorphic grade correspond to migration of the three-phase triangle of andalusite or sillimanite +

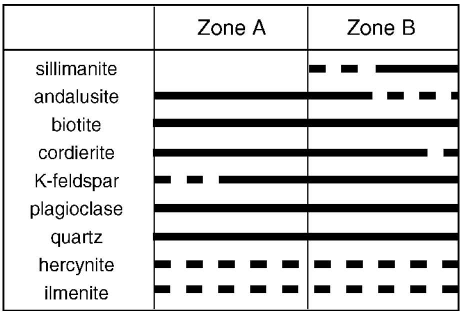

FIG. 4. Schematic mineral parageneses for the Daulet metapelites. Heavy lines show major phases and dashed lines indicate minor to trace phases.

biotite + cordierite in the AFM diagram of Thompson (1957).

After the earlier work by Albee (1965), a number of petrogenetic grids for the model pelitic KFMASH system have been proposed. Most grids explain a temperature-dependent change of mineral assemblages in kyanite-sillimanite type rocks (e.g., Appalachians: Laird, 1988). Reactions and phase relations in the andalusite-sillimanite type are different from those expected in the kyanite-sillimanite type, especially with regard to Fe-rich metapelites (Tono contact aureole, Japan: Okuyama-Kusunose, 1994; Mungyong metapelites, Korea: Ahn and Nakamura, in prep.).

Figure 7 shows possible P-T conditions of the Daulet contact metamorphism, with reaction curves pertinent to their estimation. K-feldspar first appears with andalusite within zone A prior to the appearance of sillimanite. The P-T path of the Daulet metamorphism must pass below an intersection of reaction curves of muscovite + quartz = andalusite/sillimanite + K-feldspar and andalusite = sillimanite transition, and the maximum pressure is about 2 kbar.

In addition, the computer program THERMOCALC version 2.7 with an updated version of the internally consistent thermodynamic dataset (Powell and Holland, 1994; Holland and Powell, 1998) was used for equilibria constraining temperature

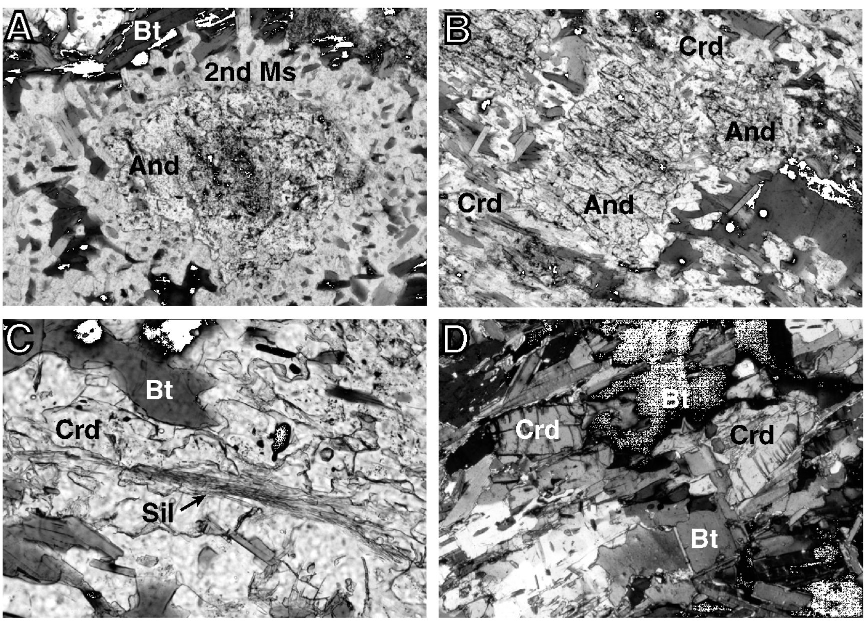

FIG. 5. Photomicrographs of Daulet metapelites. A. Polycrystalline muscovite forms a corona between an andalusite porphyroblast and biotite in T450 from zone A (plane-polarized light, length of field of view = 1.5 mm). B. Andalusite porphyroblast armored by cordierite in T414 from zone B. Some andalusite grains show simultaneous extinction (plane-polarized light, length of field of view = 1.5 mm). C. Fibrolitic sillimanite inside cordierite in T416 from zone B (plane-polarized light, length of field of view = 0.6 mm). D. Small cordierite neoblasts with biotite in T416 from zone B (crossed-polarized light, length of field of view = 1.5 mm).

TABLE 2. Representative Analyses of Biotite (O = 22) from Examined Samples

Zone:	A					B							
Sample no.:	T396	Y450	T399	Y454	Y453	Y460	Y461	T414	T416	A707	Y463	A709	
Mineral:	Bt	Bt	Bt	Bt	Bt	Bt	Bt	Bt	Bt	Bt	Bt	Bt	Bt
SiO_2	34.12	34.60	33.91	34.02	34.56	34.59	35.57	35.08	35.91	34.95	34.79	34.06	34.21
TiO_2	3.67	3.12	3.50	4.37	3.14	3.89	2.69	3.29	1.72	2.17	3.17	3.48	1.97
Al_2O_3	18.53	19.75	19.13	19.00	19.74	19.45	19.57	20.20	20.43	20.03	19.63	18.47	20.85
Cr_2O_3	0.19	0.12	0.23	0.26	0.21	0.20	0.07	0.06	0.06	0.08	0.23	0.21	0.08
FeO*	23.33	21.19	23.29	24.53	22.35	21.80	18.85	19.31	18.77	18.69	20.41	22.16	22.72
MnO	0.31	0.27	0.25	0.33	0.29	0.30	0.20	0.24	0.12	0.20	0.33	0.34	0.12
MgO	7.46	8.06	6.50	6.06	6.95	7.79	9.74	8.60	9.83	9.37	8.20	7.89	6.77
CaO	0.15	0.14	0.17	0.24	0.15	0.16	0.00	0.01	0.07	0.04	0.18	0.24	0.02
Na_2O	0.17	0.22	0.23	0.18	0.34	0.25	0.21	0.14	0.15	0.09	0.30	0.29	0.15
K_2O	10.01	9.12	10.22	9.70	9.89	9.96	10.10	10.22	9.76	10.13	10.20	10.12	9.30
Total	97.94	96.57	97.43	98.68	97.62	98.38	96.99	97.15	96.81	95.73	97.45	97.25	96.18
						Cations per 22 oxygens							
Si	5.200	5.247	5.199	5.164	5.241	5.194	5.325	5.259	5.357	5.302	5.246	5.210	5.240
Ti	0.421	0.356	0.404	0.499	0.358	0.439	0.303	0.371	0.193	0.248	0.360	0.401	0.227
Al	3.328	3.530	3.458	3.399	3.527	3.442	3.452	3.570	3.592	3.581	3.489	3.331	3.765
Cr	0.023	0.014	0.028	0.031	0.025	0.024	0.008	0.007	0.007	0.009	0.027	0.025	0.010
Fe	2.974	2.687	2.987	3.113	2.834	2.737	2.360	2.422	2.341	2.371	2.574	2.835	2.911
Mn	0.040	0.035	0.033	0.043	0.037	0.038	0.026	0.030	0.015	0.025	0.043	0.044	0.015
Mg	1.696	1.821	1.486	1.371	1.570	1.744	2.174	1.922	2.185	2.120	1.843	1.799	1.547
Ca	0.024	0.023	0.028	0.038	0.025	0.026	0.000	0.002	0.011	0.007	0.029	0.039	0.002
Na	0.051	0.065	0.067	0.052	0.101	0.072	0.060	0.041	0.044	0.025	0.089	0.085	0.045
K	1.947	1.763	1.998	1.878	1.912	1.907	1.929	1.955	1.858	1.961	1.963	1.975	1.816
Sum	15.703	15.540	15.687	15.588	15.631	15.624	15.637	15.580	15.602	15.649	15.663	15.742	15.578
XMg	0.363	0.404	0.332	0.306	0.356	0.389	0.479	0.443	0.483	0.472	0.417	0.388	0.347

[1] Total Fe as FeO.

TABLE 3. Representative Analyses of Cordierite (O = 18) and K-feldspar (0 =8) from Examined Samples

Zone:	A					B								
Sample no.:	T396	Y450	T399	Y454	Y453	Y460	Y461	T414	T416	A707	Y463	Y465	T399	Y460
Mineral:	Crd	Crd	Crd	Crd	Crd	Crd	Crd	Crd	Crd	Crd	Crd	Crd	Kfs	Kfs
SiO_2	46.38	47.51	47.22	47.72	47.30	47.71	47.87	48.20	48.17	47.23	47.45	47.63	64.00	62.91
TiO_2	0.23	0.23	0.25	0.25	0.26	0.26	0.04	0.00	0.01	0.03	0.24	0.24	0.30	0.26
Al_2O_3	31.74	32.64	32.64	32.90	32.13	33.15	32.71	33.32	32.56	32.64	32.31	32.43	18.93	18.38
Cr_2O_3	0.14	0.13	0.15	0.13	0.15	0.14	0.00	0.02	0.01	0.00	0.15	0.13	0.13	0.14
FeO[1]	12.30	12.15	12.54	11.63	12.79	11.24	9.46	9.71	9.13	9.45	10.27	10.63	0.22	0.26
MnO	0.34	0.37	0.31	0.31	0.44	0.40	0.35	0.65	0.44	0.57	0.52	0.56	0.15	0.15
MgO	6.70	6.25	6.04	5.66	5.78	6.70	7.58	7.25	7.75	7.50	6.99	6.87	0.08	0.06
CaO	0.12	0.12	0.11	0.12	0.13	0.14	0.03	0.04	0.01	0.01	0.12	0.16	0.24	0.40
Na_2O	0.79	0.30	0.22	0.97	0.23	0.25	0.21	0.26	0.26	0.25	0.23	0.25	3.75	1.18
K_2O	0.10	0.10	0.09	0.09	0.09	0.10	0.02	0.00	0.01	0.02	0.10	0.08	12.67	15.10
Total	98.84	99.79	99.56	99.76	99.31	100.08	98.28	99.44	98.36	97.70	98.38	98.97	100.46	99.63
						Cations per 18 oxygens							Cations per 8 oxygens	
Si	4.885	4.930	4.918	4.946	4.947	4.915	4.969	4.955	4.990	4.942	4.953	4.951	2.935	2.940
Ti	0.018	0.018	0.020	0.019	0.021	0.020	0.003	0.000	0.000	0.002	0.019	0.018	0.010	0.009
Al	3.939	3.991	4.006	4.019	3.961	4.024	4.003	4.037	3.976	4.025	3.975	3.973	1.023	1.013
Cr	0.011	0.010	0.013	0.011	0.012	0.011	0.000	0.001	0.001	0.000	0.013	0.011	0.005	0.001
Fe	1.083	1.054	1.092	1.008	1.119	0.969	0.821	0.835	0.791	0.827	0.897	0.924	0.008	0.010
Mn	0.031	0.033	0.027	0.027	0.039	0.035	0.031	0.057	0.039	0.050	0.046	0.049	0.006	0.006
Mg	1.052	0.966	0.937	0.874	0.901	1.029	1.173	1.111	1.196	1.169	1.088	1.064	0.005	0.004
Ca	0.014	0.013	0.013	0.013	0.015	0.015	0.003	0.004	0.001	0.002	0.014	0.017	0.012	0.020
Na	0.161	0.059	0.045	0.195	0.047	0.050	0.042	0.052	0.053	0.050	0.046	0.051	0.333	0.107
K	0.013	0.013	0.012	0.012	0.012	0.013	0.003	0.000	0.001	0.002	0.013	0.010	0.741	0.949
Sum	11.208	11.088	11.082	11.123	11.075	11.080	11.048	11.052	11.048	11.070	11.064	11.069	5.078	5.067
XMg	0.493	0.478	0.462	0.464	0.446	0.515	0.588	0.571	0.602	0.586	0.548	0.535		

*Total Fe as FeO.

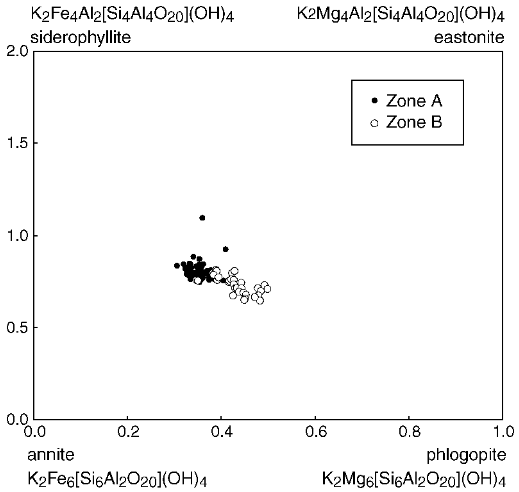

FIG. 6. Composition of biotite as plotted in the "biotite plane." Formulae: annite = $K_2Fe_6[Si_6Al_2O_{20}](OH)_4$; phlogopite = $K_2Mg_6[Si_6Al_2O_{20}](OH)_4$; siderophyllite = $K_2Fe_4Al_2[Si_4Al_4O_{20}](OH)_4$; eastonite = $K_2Mg_4Al_2[Si_4Al_4O_{20}](OH)_4$. Mineral formulae of biotite calculated to 22 oxygens, excluding H_2O. Total Fe is regarded as Fe^{2+}.

and pressure. Activities of mineral end-members for the THERMOCALC calculations were computed using the computer program AX, recomended by Holland and Powell (1988), for biotite (phl, ann, east), cordierite (crd, fcrd, mncrd), and K-feldspar (san, ab) following Holland and Powell (1998). Quartz was assumed to be pure, and fluid composition to be pure H_2O. Independent reactions for the THERMOCALC calculations are listed in Table 4. The THERMOCALC program with compositions of coexisting biotite, cordierite, and K-feldspar (T399 and Y460; Table 2 and 3) yielded P-T conditions of contact metamorphism in the Daulet metapelites by the solid intrusion of the Kokchetav UHP-HP unit.

Discussion

Observations in this study indicate that the heat source of metamorphism in the Daulet Suite is not the Devonian granitoid but the hot UHP-HP unit. The Daulet Suite was tectonically overlain and thermally metamorphosed by the UHP-HP unit prior to intrusion of the Devonian granitoid.

Sillimanite-bearing zone B appears as a wide zone with thickness of ~100 m in the Kulet area, but it appears only as a narrow zone with a thickness less than 50 m in the Chaglinka and Sulu-Tjube areas. Such a difference is due to the difference in metamorphic grade of the overlying UHP-HP unit; coesite occurs in the Kulet area, but does not occur in the Chaglinka and Sulu-Tjube areas. Ota et al. (2000) estimated peak conditions of eclogite from the UHP unit in the Kulet and Saldat-Kol regions, and subhorizontal thermobaric structure with the core (30 < P < 37 kbar, 500 < T < 900°C) in the structural middle (Fig. 8B). There are obvious tectonic and metamorphic discontinuities between the Daulet Suite and the Kokchetav UHP-HP unit; especially prominent is the pressure gap corre-

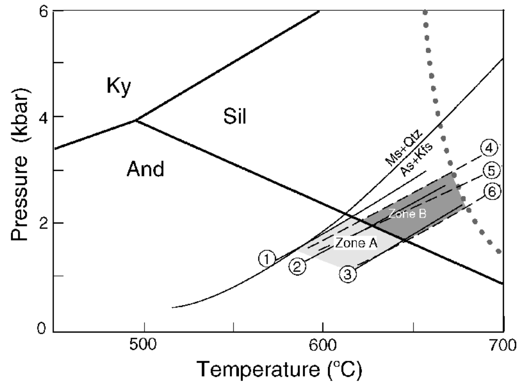

FIG. 7. Pressure-temperature diagrams of the Daulet metamorphism. The pressure and temperature conditions of metamorphism were estimated by the relation of muscovite + quartz dehydration and andalusite-sillimanite transition. Al_2SiO_5 phase relations of Holdaway (1971), muscovite + quartz dehydration reaction curve, and minimum melting of granitic composition (Luth et al., 1964) are shown by bold solid, solid, and dashed lines, respectively.

TABLE 4. Independent Reactions Used in THERMOCALC Calculations[1]

(1) 2ann + 9qz + 6and = 3fcrd + 2san + $2H_2O$
(2) east + 5qtz + and = crd + san + H_2O
(3) 2phl + 9qtz + 6and = 3crd + 2san + $2H_2O$
(4) 2ann + 9qtz + 6sill = 3fcrd + 2san + $2H_2O$
(5) east + 5qtz + sill = crd + san + H_2O
(6) 2phl + 9qtz + 6sill = 3crd + 2san + $2H_2O$

[1]Formulae of end members are after Holland and Powell (1998).

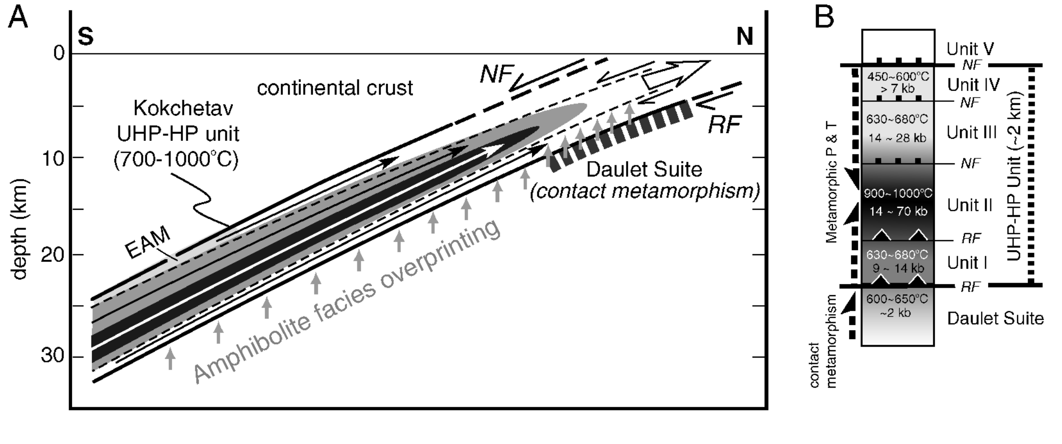

FIG. 8. Schematic model showing exhumation process of the Kokchetv UHP-HP unit. A. The tectonic intrusion of the Kokchetav UHP-HP unit into the low-pressure units. The weakly metamorphosed underlying unit is rich in hydrous phases, hence large amounts of water-rich fluid were available to modify the UHP-HP mineralogy by hydration reactions when the UHP-HP unit is thrust over by wedge extrusion. B. Pressure-temperature metamorphic conditions from the Daulet Suite and units I-IV (Ota et al., 2000).

sponding to several tens of kilometers along the boundary thrust.

The tectonic juxtaposition of a dehydrated UHP-HP unit on hydrous low-grade rocks would allow infiltration of fluids into the UHP-HP unit (Fig. 8A). Such a tectonic overlap would transport sufficient fluids from the underlying unit to the overlying UHP-HP unit, and would effectively obliterate the UHP-HP mineralogy. Accordingly, most of the ultrahigh-pressure minerals were selectively replaced by Barrovian-type assemblages. The extent of such retrogression complicates the debate on the exotic versus coherent origin of coesite-bearing rocks enveloped by gneiss with the Barrovian-type mineralogy (e.g. Tabata et al., 1998).

The degree of dehydration in the Daulet Suite by contact metamorphism was estimated by measurement of ignition loss for selected samples from zones A and B. Highly to moderately altered samples were excluded from the measurement. Figure 9 shows frequency diagrams of the ignition loss for selected samples. The peak and average value of ignition loss decrease with metamorphic grade, the latter decreasing from 2.9 wt% in zone A to 2.3 wt% in zone B. This result suggests that the degree of dehydration increases with metamorphic grade, so that the UHP-HP rocks may have been hydrated by the fluids along the thrust. The thickness of zone B varies by areas, but it can be estimated that ~668 cm^3 of aqueous fluids were released per square centimeter in the case of 100 m thickness of the Daulet Suite.

Many UHP-HP rocks were partially hydrated during exhumation, and are overprinted by Barrovian-type metamorphism. Fluids from a subducting slab will exert important effects on metasomatic and melting relations in the overlying crust or mantle wedge (Selverstone et al., 1984, 1992). If the rates of ascent of UHP-HP rocks were slow after the juxtaposition with low-P/T hydrous rocks, the UHP-HP mineral assemblages could be completely obliterated by metamorphic overprinting and/or partial melting. Preserving UHP-HP mineral assemblages requires rapid exhumation and cooling in order not to promote hydration reactions under crustal P-T conditions. The extensive hydration reactions in the known UHP metamorphic belts, including the Kokchetav massif, suggest that the rates of ascent have not been rapid enough to preserve the deep-seated mineral assemblages during exhumation. U-Pb ages of zircons with overgrowth zoning from the Daulet metapelites can reveal timing of the juxtaposition, and the difference in age from the peak metamorphism of the UHP-HP unit allows us to estimate the exhumation rates of the UHP-HP unit. Katayama et al. (2001) examined zoning and mineral inclusions in zircon from the Kokchetav diamond-bearing UHP gneisses and the Daulet pelitic

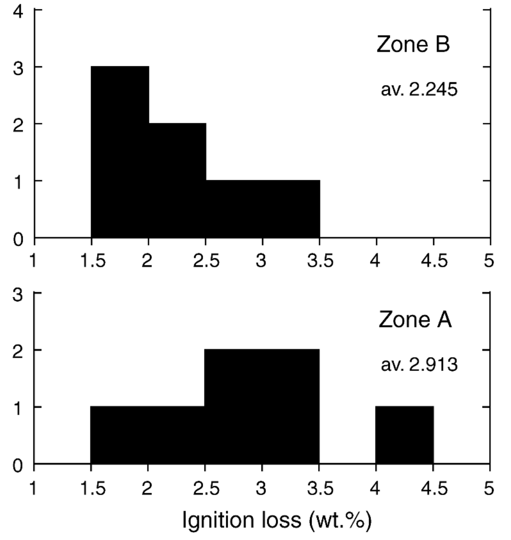

FIG. 9. Frequency diagrams of ignition loss in metapelites from zones A and B.

schist, and reported SHRIMP U-Pb ages for peak and post-peak stages of metamorphism from zoned zircons. Their SHRIMP data identified discrete ages: 539 ± 9 Ma for the UHP conditions, 507 ± 8 Ma for the late-stage amphibolite-facies overprinting, and 456–461 Ma for the post-orogenic thermal events, which yielded relatively rapid exhumation rates of ~5 km/Ma.

Slab break-off and the resultant buoyancy of a low-density continental sheet caused a wedge extrusion exhuming coesite- and diamond-facies supracrustal rocks from mantle depths up to crustal depths, exposing them at the surface in a collision suture (Maruyama et al., 1996). These authors showed that a high-P/T unit is sandwiched between the overlying and underlying units, recrystallized at 2 to 3 kbar for B-type and 5 to 6 kbar for A-type terranes. The Kokchetav massif is an A-type terrane, but the depth of the tectonic juxtaposition is shallow like a B-type terrane.

Conclusions

Metapelitic rocks in the andalusite-sillimanite type Daulet contact metamorphism provide a good opportunity to reveal a new type of metamorphism. (1) The underlying Daulet Suite was metamorphosed by the solid intrusion of the hot Kokchetav UHP-HP unit. (2) P-T conditions of the Daulet metamorphism were 580 to 680°C at nearly constant pressures of about 2 kbar; the tectonic juxtaposition occurred at shallow crustal levels. (3) The tectonic juxtaposition of a dehydrated UHP-HP unit on a hydrous weakly metamorphosed unit transported substantial amounts of fluid from the underlying unit to the overlying UHP-HP unit.

Acknowledgments

We are deeply indebted to M. J. Holdaway and A. El-Shazly for their critical reviews and constructive comments. Field survey and collection of rock samples used in this study were carried out with S. Maruyama, C. D. Parkinson, M. Ishikawa, R. Anma, J. G. Liou, Y. Ogasawara, Y. Nakajima, I. Katayama, H. Yamauchi, and J. Yamamoto, who are gratefully acknowledged. We would like to express our gratitude to the staff of Nedra Geological Expedition, Kazakhstan, for the assistance at field work. We would like to thank H. Ozawa at Naruto University of Education for making available that institution's microprobe. This study was financially supported in part by a project on Whole Earth's Dynamics from the Science and Technology Agency of Japan and by a Grant-in-Aid of the Ministry of Education, Science, Sports, and Culture of Japan (No. 12640445/M.T.).

REFERENCES

Albee, A. L., 1965, A petrogenetic grid for the Fe-Mg silicates of pelitic schists: American Journal of Science, v. 263, p. 512–536.

Dobretsov, N. L., Sobolev, N. V., Shatsky, V. S., Coleman, R. G. and Ernst, W. G., 1995, Geotectonic evolution of diamondiferous paragneisses, Kokchetav Complex, northern Kazakhstan: The geologic enigma of ultrahigh-pressure crustal rocks within a Paleozoic fold belt: The Island Arc, v. 4, p. 267–279.

England, P., and Molnar, P., 1993. The interpretation of inverted metamorphic isograds using simple physical-calculations: Tectonics, v. 12, 145–157.

Gansser, A., 1964, Geology of the Himalayas. London, UK, Interscience, 289 p.

Hodges, K. V., Parrish, R. R., and Searle, M. P., 1996, Tectonic evolution of central Annapurna Range, Nepalese Himalayas: Tectonics, v. 15, p. 1264–1291.

Holdaway, M. J., 1971, Stability of andalusite and the aluminum silicate phase diagram: American Journal of Science, v. 271, p. 97–131.

Holland, T. J. B., and Powell, R., 1998, An internally consistent thermodynamic data set for phases of petrological interest: Journal of Metamorphic Geology, v. 16, p. 309–343.

Ishikawa, M., Kaneko, Y., Anma, R., and Yamamoto, H., 2000, Subhorizontal boundary between ultrahigh-pressure and low-pressure metamorphic units in the Sulu-Tjube area of the Kokchetav Massif, Kazakhstan: The Island Arc, v., 9, p. 317–328.

Kaneko, Y., 1997, Two-step exhumation model of the Himalayan Metamorphic Belt, central Nepal: Journal of the Geological Society of Japan, v. 103, p. 203–226.

Kaneko, Y., Maruyama, S., Terabayashi, M., Yamamoto, H., Ishikawa, M., Anma, R., Parkinson, C. D., Ota, T., Nakajima, Y., Katayama, I., Yamamoto, J., and Yamauchi, K., 2000, Geology of the Kokchetav UHP-HP metamorphic belt: The Island Arc, v. 9, p. 269–283.

Katayama, I., Maruyama, S., Parkinson, C. D., Terada, K., and Sano, Y., 2001, Ion micro-probe U-Pb zircon geochronology of peak and retrograde stage of ultrahigh-pressure metamorphic rocks from the Kokchetav massif, northern Kazakhstan: Earth and Planetary Science Letters, v. 5831, p. 1–14.

Kretz, R., 1983, Symbols for rock-forming minerals: American Mineralogist, v. 73, p. 216–233.

Le Fort, P., 1975, Himalayas, the collided range: Present knowledge of the continental arc: American Journal of Science, v. 275, p. 1–44.

______, 1986, Metamorphism and magmatism during Himalayan collision: Geological Society of London, Special Publication 19, p. 159–172.

Laird, J., 1988, Arenig to Wenlock age metamorphism in the Appalachians, *in* Harris, A. L., and Fettes, D. J., eds., The Caledonian–Appalachian Orogen: Geological Society of London Special Publication 38, p. 311–345.

Luth, W. C., Jahns, R. H., and Tuttle, O. F., 1964, The granite system at pressures of 4 to 10 kilobars: Journal of Geophysical Research, v. 69, p. 759–773.

Maruyama, S., Liou, J. G., and Terabayashi, M., 1996, Blueschists and eclogites of the world and their exhumation: International Geology Review, v. 38, p. 490–596.

Okuyama-Kusunose, Y., 1994, Phase relations in andalusite-sillimanite type Fe-rich metapelites: Tono contact metamorphic aureole, northeast Japan: Journal of Metamrophic Geology, v. 12, p. 153–168.

Ota, T., Terabayashi, M., Parkinson, C. D., and Masago, H., 2000, Thermobaric structure of the Kokchetav untrahigh-pressure-high-pressure massif deduced from a north-south transect in the Kulet and Saldat-Kol regions, northern Kazakhstan: The Island Arc, v. 9, p. 328–357.

Oxburgh, E. R., and Turcotte, D. L., 1974, Thermal gradients and regional metamorphism in overthrust terrains with special reference to the eastern Alps: Schweizerische Mineralogische und Petrographische Mitteilungen, v. 54, p. 641–662.

Powell, R., and Holland, T. J. B., 1994, Opticalgeothermometry and geobarometry: American Mineralogist, v. 79, p. 120–133.

Selverstone, J., Franz, G., Thomas, S., and Getty, S., 1992, Fluid variability in 2 GPa eclogites as an indicator of fluid behavior during subduction: Contributions to Mineralogy and Petrology, v. 112, p. 341–357.

Selverstone, J., Spear, F. S., Franz, G., and Morteani, G., 1984, High-pressure metamorphism in the SW Tauern Window, Austria: P/T paths from hornblende-kyanite-staurolite schists: Journal of Petrology, v. 2, p. 501–531.

Shatsky, V. S., Sobolev, N. V., and Vavilov, M. A., 1995, Diamond-bearing metamorphic rocks of the Kokchetav massf (northern Kazakhstan), *in* Coleman, R. G., and Wang, X., eds., Ultrahigh-pressure metamorphism: Cambridge, UK, Cambridge University Press, p. 425–455.

Tabata, H., Yamauchi, K., Maruyama, S., and Liou, J. G., 1998, Tracing the extent of a UHP metamorphic terrane: Mineral inclusion study of zircons in gneisses from the Dabie Shan, *in* Hacker, B. R., and Liou, J. G., eds., When continents collide: Geodynamics and geochemistry of ultrahigh-pressure rocks: Amsterdam, Netherlands, Kluwer Academic Publishers, p. 261–273.

Terabayashi, M., 1999, The Daulet metamorphism: A contact metamorphism by solid intrusion of UHP-HP metamorphic slab [abs], *in* Superplume International Workshop Abstracts, p. 125–126, Wako, Japan.

Thompson, J. B., Jr., 1957, The graphical analysis of mineral assemblages in pelitic schists: American Mineralogist, v. 42, p. 842–858.

Yamamoto, H., Ishikawa, M., Anma, R., and Kaneko, Y., 2000, Kinematic analysis of UHP-HP metamorphic rocks in Chaglinka-Kulet area of the Kokchetav complex, central Asia: The Island Arc, v. 9, p. 304–316.

Yardley, B. W. D., 1989, An introduction to metamorphic petrology: London, UK, Longman Scientic & Technical, 248 p.